Slowdown of the meridional overturning circulation in the upper Pacific Ocean

Michael J. McPhaden* **& Dongxiao Zhang*‡**

* *NOAA/Pacific Marine Environmental Laboratory, Seattle, Washington 98115, USA*
‡ *Joint Institute for the Study of the Atmosphere and Ocean, University of Washington, Seattle, Washington 98115, USA*

Decadal temperature fluctuations in the Pacific Ocean have a significant effect on marine ecosystems and the climate of North America. The physical mechanisms responsible for these fluctuations are poorly understood. Some theories ascribe a central role to the wind-driven meridional overturning circulation between the tropical and subtropical oceans. Here we show, from observations over the past 50 years, that this overturning circulation has been slowing down since the 1970s, causing a decrease in upwelling of about 25% in an equatorial strip between 9° N and 9° S. This reduction in equatorial upwelling of relatively cool water, from 47×10^6 to 35×10^6 m^3 s^{-1}, is associated with a rise in equatorial sea surface temperatures of about 0.8 °C. Another effect of the slowing circulation is a reduction in the outgassing of CO_2 from the equatorial Pacific Ocean—at present the largest oceanic source of carbon dioxide to the atmosphere.

Recent analyses of historical data have revealed the signatures of decadal-timescale variations in the ocean–atmosphere system of the Pacific basin. These variations have been characterized in terms of cyclic oscillations over a broad band of frequencies with periods between 10 and 70 years[1]. Alternatively, they have been described in terms of regime shifts—abrupt and coherent changes in climatological conditions affecting large areas of the Pacific basin—the most pronounced of which in the past 50 years occurred in 1976–77 (ref. 2). One representation of this decadal variability, the so-called Pacific Decadal Oscillation (PDO), has a spatial structure very similar to that of the El Niño/Southern Oscillation (ENSO), which fluctuates between warm (El Niño) and cold (La Niña) phases at shorter periods of 3–7 years (refs 3, 4). Like ENSO, decadal-timescale temperature fluctuations in the Pacific have substantial effects on marine ecosystems and the climate of North America[5,6]. The dynamics of decadal fluctuations are much less well understood than those of ENSO, however, and there is considerable debate about the underlying physical processes that govern them, especially in the ocean[7]. Some theories invoke mid-latitude ocean–atmosphere interactions originating in the North Pacific Ocean[8], while others point to the importance of ocean–atmosphere interactions spanning tropical and subtropical latitudes[9–11].

One of the most prominent theories for Pacific decadal climate variability[11] assumes that the meridional overturning circulation in the upper ocean acts as a conveyor belt for transporting water mass anomalies from the subtropics to the tropics. In this theory, air–sea interactions in the subtropics create surface water masses with unusually warm or cold temperatures that are subducted—that is, pushed downward—into the pycnocline (where the water density increases rapidly with depth). The temperature-tagged waters slowly drift equatorward below the surface for roughly 10 years, during which time they are isolated from further interaction with atmosphere. When these waters reach equatorial latitudes, they are upwelled to the surface where they are presumed to affect equatorial sea surface temperatures, air–sea heat exchange, and overlying atmospheric circulation in a manner similar to what happens during ENSO events. The upwelled water then flows back towards the subtropics in the surface layer to complete one circuit of the meridional circulation cell.

But recent evidence suggests that temperature anomalies subducted into the pycnocline at subtropical latitudes may not reach the Equator with any appreciable amplitude[12]. Model studies have indicated that these anomalies can be either strongly dissipated, disperse in the form of planetary-scale oceanic waves, or become obscured by wind-forced variations at low latitudes[13–15]. Thus, a related hypothesis for the role of the meridional overturning circulation in decadal-timescale climate variability has been proposed: the circulation speeds up or slows down, transporting water masses with relatively constant properties at faster or slower rates towards the Equator[16]. A dynamically changing ocean circulation has significant implications for equatorial upwelling—which affects not only tropical Pacific sea surface temperatures, but also the exchange of CO_2 across the air–sea interface and the supply of nutrients to the biologically productive surface layer of the ocean.

To address the question of whether the meridional overturning circulation in the upper Pacific may be changing on decadal timescales, we have analysed hydrographic data between 20° S and 50° N for the period 1950–99 in the depth range of the upper pycnocline (typically 50–400 m in the tropical and subtropical Pacific). We have also computed surface-layer Ekman transports using multi-decade long wind products derived from empirical and atmospheric model-based analyses of available observations. Results of our analysis, and implications for climate variability, are described below.

Mean circulation in the pycnocline

To illustrate important features of the general circulation, and to set the context for discussion of decadal variations in pycnocline flows, Fig. 1a shows the 50-year mean geostrophic streamlines and horizontal velocity field on the 25.0 kg m^{-3} potential density surface which is located in the middle of the upper pycnocline. This density surface outcrops at the sea surface between about 30° and 40° N in the Northern Hemisphere and south of 20° S (except in the far eastern Pacific) in the Southern Hemisphere. Water subducted into the pycnocline along these outcrop lines can make its way to the Equator by both interior and western-boundary routes. Interior pathways are more circuitous in the Northern Hemisphere because of the presence of a potential vorticity ridge along 9°–10° N (associated with uplift of the pycnocline under the Intertropical Convergence Zone), which tends to block the flow of waters between higher latitudes and the Equator in the eastern and central Pacific[17]. Based on our estimates of geostrophic velocity, transit times to the Equator on this density surface are about 5–10 years, depending on details of a water parcel's pathway and where it is subducted. Comparable transit times and circulation pathways have

© 2002 Macmillan Magazines Ltd

been inferred from numerical model simulations[18], circulation theory[19] and tracer distributions[20,21].

The flow pattern shown in Fig. 1a is similar to that on isopycnals between about 22 and 26 kg m^{-3} in the Northern Hemisphere and on isopycnals between 22.5 and 26.2 kg m^{-3} in the Southern Hemisphere. Waters less dense than 22.0 kg m^{-3} almost always fall within the surface mixed layer in the tropics, while interior flow on density surfaces deeper than 26.2 kg m^{-3} is weakly poleward near the Equator[17]. Thus, for the purpose of this analysis, we define interior pycnocline transports associated with the shallow meridional overturning circulation as occurring within the above range of density classes.

We calculate pycnocline transports by integrating equatorward flows along 9° N and 9° S from the eastern boundary to near the western boundary. We choose 9° N because it represents a choke point for meridional geostrophic transports in the interior ocean. No similar constriction is present south of the Equator, so we integrate along 9° S for hemispheric symmetry. To test for continuity with meridional transports from higher latitudes, we repeated these calculations at 15° N and 15° S, which approximate the boundaries separating the subtropical and tropical gyres in terms of the depth-integrated horizontal mass transport streamfunction[22].

Decadal variations in pycnocline transports

We calculated meridional mass transports for 7–10 year periods in such a way as to span the 1976–77 regime shift, and to maximize utilization of the data that are not uniformly distributed in time. As expected from previous work[17], transports are higher in the Southern Hemisphere than in the Northern Hemisphere where flow between the subtropics and tropics is more obstructed in the interior ocean (Fig. 2a). However, we find that these transports have been non-stationary, with comparable decreases of 6–7 sverdrups (1 Sv = 10^6 m^3 s^{-1}) across both 9° N and 9° S since the 1970s.

The combined equatorward transport (or convergence) of pycnocline water across 9° N and 9° S drops from 27.0 ± 2.5 Sv before the regime shift in the 1970s to 14.0 ± 1.5 Sv in the 1990s (Table 1). For comparison, meridional transport convergences decrease from 38.0 ± 1.8 Sv in the 1970s to 29.5 ± 1.9 Sv in the 1990s across 15 °N and 15° S in the same density classes. Larger absolute transports are expected at 15 °N and 15° S because some of the interior ocean transport crossing the gyre boundaries is eventually shunted into equatorward-flowing western boundary currents. However, the downward trend is similar in magnitude to that observed across 9° N and 9° S, and is likewise the result of approximately equal decreases in Northern and Southern Hemisphere transports. Differences in the downward trend (8.5 Sv across 15° versus 13 Sv across 9°) may in part be due to the fact that some of the very lightest waters between 22 and 23 kg m^{-3} are formed equatorward of 15 °N and 15° S. Decadal changes in western boundary current transports between 9° and 15° may also account for some of the difference, though (as will be shown below) changes in these transports of only a few sverdrups are not detectable with confidence from our analysis.

The period from the 1970s to the 1990s coincides with a rise in sea surface temperatures of about 0.8 °C in the equatorial Pacific[4] (Fig. 2b). This temperature increase cannot be explained by an increase in surface heating. On the contrary, heat fluxes into the ocean have decreased over the past 50 years in the equatorial Pacific, primarily owing to an increase in cloudiness that has reduced the amount of sunlight reaching the surface[23]. Thus, as occurs on ENSO timescales, changes in surface heat flux act to damp rather than to generate decadal changes in equatorial sea surface temperatures.

What accounts for the observed decadal decreases in interior

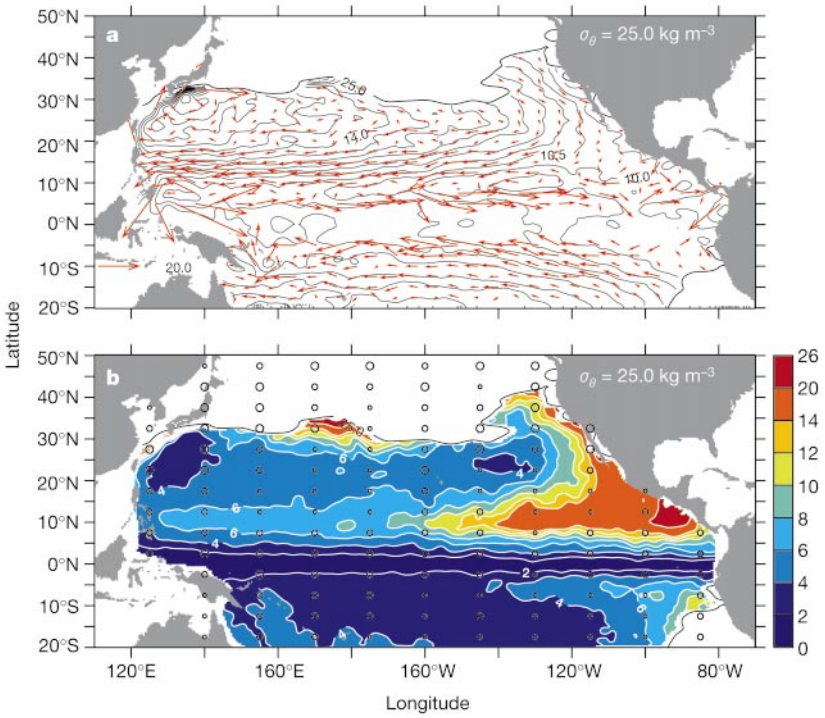

Figure 1 Mean circulation and potential vorticity averaged over 50 years (1950–99) in the upper pycnocline of the Pacific Ocean. **a**, Geostrophic streamlines relative to 900 dbar (in m^{-2} s^{-2}) and **b**, absolute value of potential vorticity (in 10^{-10} m^{-1} s^{-1}) on the 25.0 kg m^{-3} potential density surface. Velocity vectors are overplotted on **a**. Distribution of hydrocasts down to 900 dbar is overplotted on **b**, with the size of the dots representing total number of casts in regions of 5° latitude by 15° longitude (smallest, 50–300; intermediate, 301–1,000; largest, 1,001 or more). Winter season outcrop lines are drawn in both panels. The outcrop lines define locations where wintertime surface mixing penetrates deepest into the pycnocline, creating new water masses that are subsequently sequestered from the atmosphere as seasonal heating restratifies the upper ocean in spring and summer. Potential vorticity is defined as $f(\partial\rho/\partial z)/\rho_0$, where f is the Coriolis parameter, $\partial\rho/\partial z$ is the vertical density gradient, and ρ_0 is a constant reference density (10^3 kg m^{-3}). Water parcels conserve their potential vorticity in an ideal fluid.

© 2002 Macmillan Magazines Ltd

ocean geostrophic transports, and are they related to the increases in sea surface temperature? Comparing the periods 1970–77 and 1990–99, we see that associated with the increase in sea surface temperature there is a decrease in the intensity of the easterly trade winds, as indicated by the prevalence of persistent westerly wind stress anomalies in the central and western Pacific (Fig. 3a). These features are the tropical manifestation of the PDO in its 'high' phase (warm tropics, cold central North Pacific)[3,4]. Weaker surface easterlies in the 1990s are accompanied by increased surface wind convergence, atmospheric deep convection, and rainfall in the central equatorial Pacific, similar to what occurs during El Niño events[24].

The pycnocline normally slopes down to the west near the Equator, under the influence of easterly trade wind forcing. This pycnocline slope induces a geostrophically balanced meridional inflow towards the Equator in both hemispheres. The pattern of wind stress differences in Fig. 3a favours a relaxation of this pycnocline tilt, with anomalous deepening in the east and shoaling in the west. Consistent with this expectation, the depth of the pycnocline (as indicated by 25.0 kg m^{-3} surface) becomes shallower by about 10–30 m west of 160° W and deeper by about 10–30 m between 120°–150° W in the 1990s relative to the 1970s (Fig. 3b). As a consequence, equatorward geostrophic transport is reduced in both hemispheres in the 1990s, in accordance with ocean circulation theory that predicts less interior pycnocline exchange for anomalous westerly winds near the Equator[25].

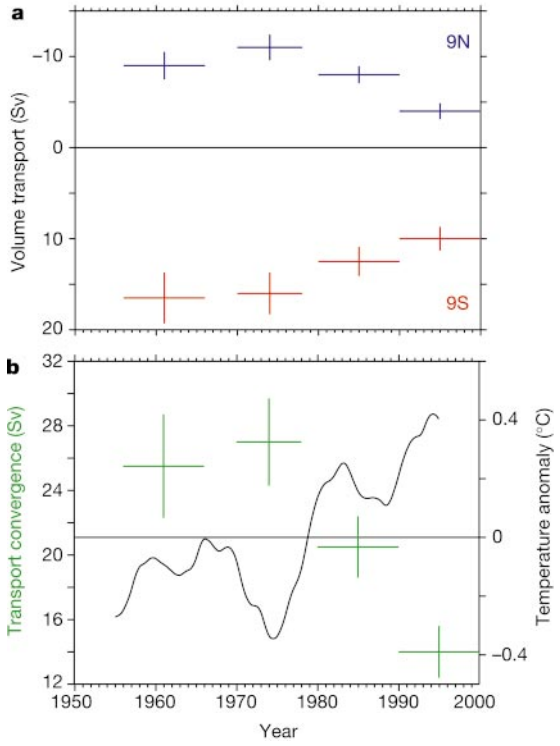

Figure 2 Meridional transports in the pycnocline and smoothed sea surface temperatures over the past 50 years. **a**, Mean zonally integrated meridional transports in the pycnocline relative to 900 dbar along 9° N and 9° S, computed for 1956–65, 1970–77, 1980–89 and 1990–99. Values are integrated in the Northern Hemisphere from the eastern boundary to 145° E in density classes between 22 and 26 kg m^{-3}, and in the Southern Hemisphere from the eastern boundary to 160° E in density classes between 22.5 and 26.2 kg m^{-3}. Transports are in units of sverdrups (1 Sv = 10^6 m^3 s^{-1}) which is the volumetric equivalent of mass for a constant reference density. Error bars are for one standard error. **b**, Mean meridional transport convergence (in Sv) in the pycnocline across 9° N and 9° S. Convergence is calculated as the difference between Southern Hemisphere minus Northern Hemisphere transports in **a**. Also plotted in **b** are areally averaged sea surface temperature anomalies in the eastern and central equatorial Pacific (9° N–9° S, 90° W–180° W) where equatorial upwelling is most intense[31]. The temperature time series is derived from monthly analyses[50] smoothed twice with a 5-year running mean to filter out the seasonal cycle and year-to-year oscillations associated with ENSO. Anomalies are relative to 1950–99 averages.

Decadal variations in surface layer transports

We expect that reduced meridional convergence in pycnocline transports should be associated with reduced poleward transport of water in the surface layer. To test this hypothesis, we computed meridional Ekman transports integrated from the eastern boundary to the western boundary of the Pacific for four different wind stress products that span at least two decades. Meridional Ekman transport per unit longitude is given by the expression $M_e = -\tau^x/\rho_0 f$, where τ^x is the zonal component of the wind stress, f is the Coriolis parameter (twice the local vertical component of the Earth's angular velocity), and ρ_0 is a constant reference density (10^3 kg m^{-3}). These transports are confined approximately to the upper 50 m in the tropical oceans[26], and are to the right of the wind stress in the Northern Hemisphere and to the left of the wind stress in the Southern Hemisphere.

Most wind stress products individually show decreases in zonally integrated Ekman transports in the tropical Pacific associated with the broad-scale weakening of the trade winds between the 1970s and 1990s. However, to reduce the effects of uncertainties in individual products, and because no product is unambiguously superior, we computed ensemble means of Ekman transports and transport divergences from the four products for the same periods as for the meridional pycnocline transports in Fig. 2. Ensemble means and standard errors for the Ekman transport divergences across 9° N and 9° S, computed as $\int[M_e(9°\,\mathrm{N}) - M_e(9°\,\mathrm{S})]\,dx$, are 53.9 ± 5.3 Sv (1956–65), 58.4 ± 4.2 Sv (1970–77), 52.9 ± 4.5 Sv (1980–89) and 45.9 ± 5.5 Sv (1990–99). The Ekman transport divergence is highest during 1970–77 and lowest during 1990–99, decreasing by about 12 Sv over this time. This decrease is comparable to our estimated decrease in interior pycnocline transport convergence.

The difference between surface-layer transport divergence and pycnocline transport convergence across 9° N and 9° S should reflect flow in the western boundary currents (specifically, in the equatorward-flowing Mindanao Current across 9° N, and in the New Guinea Coastal Current and Undercurrent across 9° S). Inferred western boundary current transport convergences, estimated as the residual of a mass balance for each decadal period, are typically around 25 Sv (Table 1). Several more sverdrups at minimum should be added to these convergences, as western boundary currents (and the Mindanao Current in particular) supply upper pycnocline waters to feed much of the flow that exits the Pacific basin into the Indian Ocean through the Indonesian straits[27]. It is noteworthy, though, that these western boundary transport convergences, whose magnitudes are broadly consistent with those from modelling and observational studies[17,18], do not seem to vary significantly on decadal timescales given the confidence limits of our estimates. Thus, if changes in western boundary current transports have

Table 1 Water mass balance for the equatorial strip between 9° N and 9° S in the Pacific

	Year range			
	1956–65	1970–77	1980–89	1990–99
Surface layer divergence (Sv)	44.8 ± 5.3	51.7 ± 4.2	47.5 ± 4.5	40.7 ± 5.5
Interior ocean pycnocline convergence (Sv)	25.5 ± 3.0	27.0 ± 2.5	20.5 ± 1.6	14.0 ± 1.5
Western boundary convergence (Sv)	19.3 ± 6.1	24.7 ± 4.9	27.0 ± 4.8	26.7 ± 5.7
Equatorial upwelling (Sv)	40.9 ± 5.7	46.8 ± 4.6	42.1 ± 4.2	35.4 ± 4.8

Values shown are mean transport convergences and divergences, plus and minus one standard error. Convergence is computed as 9° S minus 9° N transports, and divergence as 9° N minus 9° S transports. Surface-layer divergence is based on Ekman transports reduced by opposing surface layer geostrophic transports.

© 2002 Macmillan Magazines Ltd

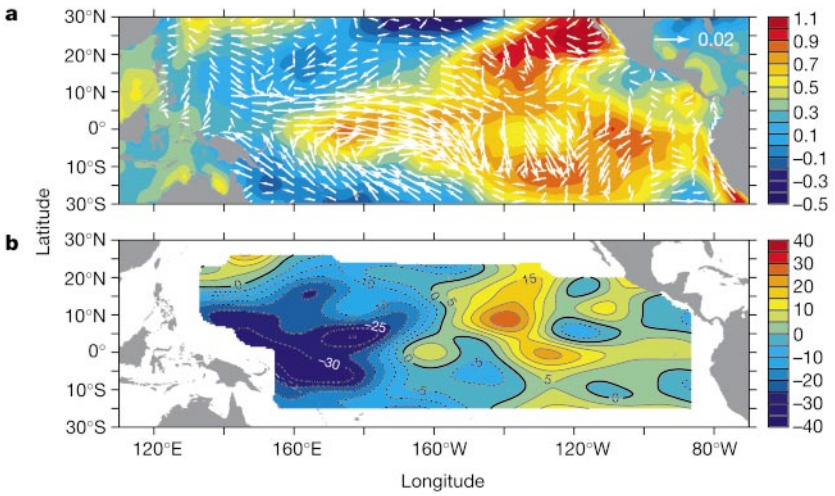

Figure 3 Decadal differences in the tropical Pacific between 1990–99 and 1970–77. **a**, Wind stress difference (in N m^{-2}) for 1990–99 minus 1970–77, based on the Florida State University wind product[44]. Overplotted is the difference in sea surface temperature (in °C) the same time period[50]. **b**, Depth difference (in m) of the 25.0 kg m^{-3} potential density surface for 1990–99 minus 1970–77.

occurred over the past several decades, they are likely to have been smaller than those for interior ocean geostrophic transports and surface-layer Ekman transports.

Comparison with Sverdrup theory

A complementary perspective on decadal variations in ocean pycnocline transports is available from Sverdrup theory[22], the dynamics of which are fundamental to our understanding of large-scale oceanic circulation. This theory assumes that flow away from western boundaries is linear and in steady-state balance with surface wind stress forcing. The steady-state assumption is valid for the tropical oceans on decadal timescales, as the adjustment time in response to transient wind forcing at low latitudes is on the order of a few years[28].

Geostrophic transport per unit longitude based on Sverdrup theory is given by $M_g = (\rho_0\beta)^{-1}[\nabla \times \boldsymbol{\tau} + \beta\tau^x/f]$, where $\boldsymbol{\tau}$ is wind stress vector and β is the change in the Coriolis parameter with latitude[19]. Using this expression, we computed meridional transport convergences, integrated from the eastern boundary to just outside the western boundary along 9° N and 9° S, for each wind stress product. Resultant ensemble averages and standard errors are 24.2 ± 2.6 Sv (1956–65), 27.1 ± 6.8 Sv (1970–77), 22.3 ± 4.9 Sv (1980–89) and 10.5 ± 4.1 Sv (1990–99). These estimates are comparable in magnitude to pycnocline transport convergences computed independently from hydrographic data, and exhibit a similar downward trend from the 1970s to the 1990s (Table 1).

Sverdrup theory provides no information about the vertical structures of geostrophic currents, so that exact comparison with observations would require integration of measured geostrophic flow over the entire water column. It is possible therefore that the good agreement between observed pycnocline transports and geostrophic transports predicted from Sverdrup theory may be fortuitous. However, the circulation in the tropical Pacific is most vigorous in the upper ocean[29], which leads us to conclude that the trend towards a weaker meridional overturning circulation from the 1970s to the 1990s is real.

Consequences for equatorial upwelling

Poleward flow in the surface Ekman layer extends to depths of about 50 m, whereas the pycnocline flows that we have identified extend to depths of hundreds of metres. The meridional overturning circulation is closed at low latitudes by upwelling, which brings cold pycnocline water to the surface where it once again makes contact with the atmosphere. Most of the upwelling transport (90% or more) in the tropical Pacific occurs along the Equator in the eastern and central basin, with smaller amounts in the Costa Rica dome (centred near 10° N, 90° W) and in the coastal upwelling regime off Peru[30]. Most of the upwelled water is of extratropical origin, although a portion is associated with shallow meridional recirculation cells confined to within a few degrees of the Equator[25,29]. Some water upwelled near the Equator downwells around 3°–4° N and 3°–4° S, returning to the Equator at the base of the surface layer. These surface-layer recirculating transports are averaged out of our estimates, which are representative of the deeper water masses of subtropical origin flowing across 9° N and 9° S.

From mass continuity, we can infer that upwelling has transported pycnocline water toward the surface between 9° N and 9° S at an average rate of about 40 Sv over the past several decades. The magnitude of this transport corresponds well with previous estimates, although different latitude and longitude ranges for the various computations preclude exact comparison[20,31,32]. Our results also indicate that these upwelling transports have varied decadally, decreasing by about 25% from 47 Sv in the 1970s to 35 Sv in the 1990s (Table 1). The reduction in upwelling is consistent with inferences from radiocarbon data of a decreased supply of pycnocline water to the surface layer in the eastern and central equatorial Pacific since the 1970s[33].

Implications for climate variability and climate change

The picture that emerges from this analysis is that the wind-driven meridional overturning circulation in the upper Pacific Ocean has been slowing down since the 1970s. This slowdown can account for the recent anomalous surface warming in the tropical Pacific, as the supply of cold pycnocline water originating at higher latitudes to feed equatorial upwelling has decreased. The Southern Hemisphere is responsible for about half of the observed decrease in equatorward pycnocline transport. Thus, perspectives on decadal variability limited to the Northern Hemisphere alone are incomplete. The fact that few studies have considered a role for the Southern Hemisphere ocean is presumably a consequence of limited data availability rather than a lack of decadal signal in the southern tropics and subtropics[34].

The oceanic and atmospheric processes that we have described work together so as to reinforce each other, similar to the positive feedbacks that occur during ENSO events. For example, weaker easterly trade winds in the equatorial Pacific would result in reduced

© 2002 Macmillan Magazines Ltd

Ekman and geostrophic meridional transports, reduced equatorial upwelling, and warmer equatorial sea surface temperatures. Warmer surface temperatures in turn would alter patterns of deep atmospheric convection so as to favour weaker trade winds. If the system is to oscillate on decadal timescales, then delayed negative feedback mechanisms, one candidate for which involves planetary-scale ocean waves, must also be important[4,16,35].

Similarities in the spatial structures of the PDO and ENSO (both, for example, have phases that are characterized by warm tropics and a cool central North Pacific, and vice versa) have raised questions about the possible interaction between interannual- and decadal-timescale phenomena in the Pacific. In particular, since 1976–77 there have been fewer La Niña events, and more frequent, stronger, and longer-lasting El Niño events. Whether this recent change in the character of the ENSO cycle is a consequence or a cause of underlying decadal-timescale variability is unknown. It could be that the decadal changes in circulation described here operate independently from those that affect the ENSO cycle. If so, they would modify the background state on which ENSO develops, and thereby precondition interannual fluctuations to preferred modes of behaviour[36,37]. Alternatively, the observed decadal changes may simply be the low-frequency residual of random or chaotic fluctuations in tropical ocean–atmosphere interactions that give rise to the ENSO cycle itself[38]. In either case, a complete understanding of climate variability spanning interannual to decadal timescales in the Pacific basin will need to account for the slowly varying meridional overturning circulation between the tropics and subtropics.

Results of some numerical coupled ocean–atmosphere model studies suggest that the response of the tropical Pacific to greenhouse-gas forcing resembles a permanent El Niño-like condition[35,39]. Thus, it is conceivable that climate fluctuations in the tropical Pacific over the past 50 years, including the recent slowdown of the meridional overturning circulation, may have been influenced by global warming as well as by natural variability. Unfortunately, separating out the putative effects of anthropogenically forced climate change from natural variations is not possible with relatively short data records. Our analysis can, however, provide an important dynamical constraint for model studies that attempt to simulate recent observed decadal changes in the Pacific basin.

Finally, we note that the equatorial Pacific is the largest oceanic source of CO_2 to the atmosphere[40,41]. It also accounts for roughly 20% of the photosynthetically mediated new biological production in the world's oceans[30]. Upwelling of nutrient- and carbon-rich water to the sea surface is the principal reason why the equatorial Pacific is so important in global biogeochemical cycles. Consistent with a decrease in upwelling in the 1990s relative to earlier decades, the outgassing of CO_2 from the equatorial Pacific Ocean has decreased from the 1980s to the 1990s[40,41], potentially reducing the rate at which CO_2 would otherwise have accumulated in the atmosphere[41]. It is also likely (though difficult to confirm for lack of adequate data) that the supply of nutrients to the surface layer of the equatorial Pacific has decreased from the 1970s to the 1990s. A reduced nutrient supply would favour a reduction in biological productivity in the equatorial Pacific, which in turn would affect overall global rates of carbon fixation. □

Methods

Processing of hydrographic data

Hydrographic data were obtained from the World Ocean Data Base[42] augmented with data from archives of the Pacific Marine Environmental Laboratory[17]. A total of 114,691 casts between 20° S and 50° N reach 900 dbar (1 dbar = 0.992 m depth), which is the reference level of our geostrophic velocity estimates. The number of casts for defining water mass properties on shallow density surfaces is greater (for example, 215, 993 casts on the 25.0 kg m^{-3} isopycnal shown in Fig. 1). By decade, the number of casts to 900 dbar is 11,584 (1950–59), 21,779 (1960–69), 24,920 (1970–79), 36,110 (1980–89) and 20,298 (1990–99).

Data coverage is relatively sparse in the Southern Hemisphere, which limits our analysis to latitudes north of 20° S. Data are also unevenly distributed spatially and temporally, potentially aliasing interannual, seasonal and shorter timescale and space-scale fluctuations into the decadal climate signals in which we are interested. Despite these sampling limitations, the data are adequate to define robust features of the mean circulation and its large-scale variability averaged over periods of 7–10 years.

Data were binned in boxes of 0.5° latitude by 0.5° longitude, then gridded objectively by decade on density surfaces. We assumed a gaussian correlation structure function with a half-width of 5° latitude by 15° longitude in the interior ocean, and 5° latitude by 5° longitude near the western boundary. The distribution of hydrocast data on the larger of these scales is shown in Fig. 1b. Our choice of 900 dbar as a reference level for geostrophic velocity computations is consistent with previous analyses in the tropical and subtropical Pacific[17]. This level represents a compromise between optimizing data coverage (which is better near to the surface) and capturing weak horizontal flows below 900 dbar. Choosing alternative reference depths (for example, 600 dbar or 1,200 dbar) leads to only minor differences in pycnocline transport values (0.5–1 Sv).

The zonal integral of interior ocean meridional geostrophic transport is effectively the difference between depth-integrated dynamic height at opposite ends of the basin. To estimate the random sampling error for these transports, we performed Monte Carlo simulations on subsets of data near the eastern and western limits of the basin for each decadal period. Typically hundreds of data pairs were available for these assessments within several degrees of latitude and longitude around the end points of the transport calculation. Results are shown as one standard error in text, figures and tables.

Ekman and Sverdrup transports

We use four wind products to compute Ekman and Sverdrup transports: the Comprehensive Ocean Atmosphere Data Set (COADS) winds for 1950–93[43], the Florida State University (FSU) winds for 1961–99[44], the National Centers for Environmental Prediction (NCEP) winds for 1958–99[45], and the European Centre for Medium Range Weather Forecasts (ECMWF)[46] winds for 1979–99. COADS provides a stress product directly; FSU, NCEP and ECMWF wind analyses were converted to wind stress using essentially the same algorithm as used in COADS. We required a minimum of 5 years in any given period to compute a decadal average.

There are shortcomings in these (and other) wind products in terms of potential systematic biases related to data coverage, analysis procedures, or both[23,47]. Therefore, rather than rely on any one product alone, we formed ensemble means of the different products to draw out significant climate signals common to all. This procedure also provides a measure of the uncertainty (in the form of statistically derived standard errors) in our representation of those signals.

Data shown in Table 1

Interior ocean pycnocline transports relative to 900 dbar were derived from hydrographic data, and convergence was computed as the difference of 9° S minus 9° N values. Ekman transports were adjusted downward for measured equatorward geostrophic flows in the surface layer of the interior ocean, and divergence computed as the difference of 9° N minus 9° S. Western boundary current transport convergences represent the difference between surface-layer divergences and interior ocean pycnocline convergences, assuming that mass is conserved in the upper ocean. Upwelling transports between 9° N and 9° S were computed by assigning 80% of the western boundary current transport convergence to the pycnocline layer and 20% to the surface layer, based on observed mean vertical structures of these currents.

Western boundary current transport convergences in Table 1 represent lower bounds, because these currents also supply upper pycnocline water to the Indonesian throughflow[27]. However, those additional sverdrups of boundary current transport required to feed the throughflow, since they simply leave the basin, do not affect our equatorial upwelling computations. Moreover, we estimate that on decadal timescales the Indonesian throughflow has remained constant to within about ±1 Sv on the basis of calculations using Godfrey's island rule[48] forced by global NCEP[45] and ECMWF[46] wind fields. Coupled ocean–atmosphere model integrations indicate a similar range of possible decadal-timescale variations in Indonesian throughflow[49]. These fluctuations are much smaller than those associated with the meridional overturning circulation in the upper Pacific.

Received 7 August; accepted 7 December 2001.

1. Minobe, S. Spatio-temporal structure of pentadecadal variability over the North Pacific. *Prog. Oceanogr.* **47,** 381–408 (2000).
2. Trenberth, K. E. & Hurrell, J. W. Decadal atmosphere-ocean variations in the Pacific. *Clim. Dyn.* **9,** 303–319 (1994).
3. Mantua, N. J., Hare, S. J., Zhang, Y., Wallace, J. M. & Francis, R. C. A Pacific interdecadal oscillation with impacts on salmon production. *Bull. Am. Meteorol. Soc.* **76,** 1069–1079 (1997).
4. Zhang, Y., Wallace, J. M. & Battisti, D. S. ENSO-like interdecadal variability: 1900–93. *J. Clim.* **10,** 1004–1020 (1997).
5. Hare, S. R. & Mantua, N. Empirical evidence for North Pacific regime shifts in 1977 and 1989. *Prog. Oceanogr.* **47,** 103–145 (2000).
6. Cayan, D. R., Kammerdiener, S. A., Dettinger, M. D., Caprio, J. M. & Peterson, D. H. Changes in the onset of spring in the western United States. *Bull. Am. Meteorol. Soc.* **82,** 399–415 (2001).
7. Miller, A. J. & Schneider, N. Interdecadal climate regime dynamics in the North Pacific Ocean: theories, observations, and ecosystem impacts. *Prog. Oceanogr.* **47,** 355–379 (2000).
8. Latif, M. & Barnett, T. P. Cause of decadal variability over the North Pacific and North America: Dynamics and predictability. *J. Clim.* **9,** 2407–2423 (1996).
9. Lindsey, B. K., Wellington, G. M. & Schrag, D. P. Decadal sea surface temperature variability in the subtropical South Pacific from 1726 to 1997 A. D. *Science* **290,** 1145–1148 (2001).

© 2002 Macmillan Magazines Ltd

10. Garreaud, R. E. & Battisti, D. S. Interannual (ENSO) and interdecadal (ENSO-like) variability in the Southern Hemisphere tropospheric circulation. *J. Clim.* **12,** 2113–2123 (1999).
11. Gu, D. & Philander, S. G. H. Interdecadal climate fluctuations that depend on exchanges between the tropics and extratropics. *Science* **275,** 805–807 (1997).
12. Schneider N., Miller, A. J., Alexander, A. & Deser, C. Subduction of decadal North Pacific temperature anomalies: Observations and dynamics. *J. Phys. Oceanogr.* **29,** 1056–1070 (1999).
13. Schneider, N. *et al.* Pacific thermocline bridge revisited. *Geophys. Res. Lett.* **26,** 1329–1332 (1999).
14. Liu, Z. & Shin, S.-I. On thermal ventilation of active and passive tracers. *Geophys. Res. Lett.* **26,** 357–360 (1999).
15. Nonaka, M., Xie, S.-P. & Takeuchi, K. Equatorward spreading of a passive tracer with application to North Pacific interdecadal temperature variations. *J. Oceanogr.* **56,** 173–183 (2000).
16. Kleeman, R., McCreary, J. P. & Klinger, B. A mechanism for generating ENSO decadal variability. *Geophys. Res. Lett.* **26,** 1743–1746 (1999).
17. Johnson, G. C. & McPhaden, M. J. Interior pycnocline flow from the subtropical to the equatorial Pacific Ocean. *J. Phys. Oceanogr.* **29,** 3073–3089 (1999).
18. Huang, B. & Liu, Z. Pacific subtropical-tropical thermocline water exchange in the National Centers for Environmental Prediction ocean model. *J. Geophys. Res.* **104,** 11065–11076 (1999).
19. McPhaden, M. J. & Fine, R. A. A dynamical interpretation of the tritium maximum in the central equatorial Pacific. *J. Phys. Oceanogr.* **18,** 1454–1457 (1988).
20. Quay, P. D., Stuiver, M. & Broecker, W. S. Upwelling rates for the equatorial Pacific Ocean derived from the bomb ^{14}C distribution. *J. Mar. Res.* **41,** 769–792 (1983).
21. Fine, R. A., Maillet, K. A., Sullivan, K. F. & Willey, D. Circulation and ventilation flux of the Pacific Ocean. *J. Geophys. Res.* **106,** 22159–22178 (2001).
22. Sverdrup, H. U. Wind-driven currents in a baroclinic ocean: with application to the equatorial currents of the eastern Pacific. *Proc. Natl Acad. Sci. USA* **33,** 318–326 (1947).
23. Liu, Z. & Huang, B. Cause of tropical Pacific warming trend. *Geophys. Res. Lett.* **27,** 1935–1938 (2000).
24. Wallace, J. M. *et al.* On the structure and evolution of ENSO-related climate variability in the tropical Pacific: Lessons from TOGA. *J. Geophys. Res.* **103,** 14241–14259 (1998).
25. McCreary, J. P. & Lu, P. On the interaction between the subtropical and the equatorial oceans: The subtropical cell. *Phys. Oceanogr.* **24,** 466–497 (1994).
26. Ralph, E. A. & Niiler, P. P. Wind-driven currents in the tropical Pacific. *J. Phys. Oceanogr.* **29,** 2121–2129 (1999).
27. Gordon, A. L., Susanto, R. D. & Ffield, A. Throughflow within the Makassar Strait. *Geophys. Res. Lett.* **26,** 3325–3328 (1999).
28. Philander, S. G. H. Variability of the tropical oceans. *Dyn. Atmos. Oceans* **3,** 191–208 (1979).
29. Johnson G. C., McPhaden, M. J. & Firing, E. Equatorial Pacific Ocean horizontal velocity, divergence, and upwelling. *J. Phys. Oceanogr.* **31,** 839–849 (2001).
30. Chavez, F. P. & Toggweiler, J. R. in *Upwelling in the Ocean: Modeling Processes and Ancient Records* (eds Summerhayes, C. P. *et al.*) 313–320 (Wiley, New York, 1995).
31. Wyrtki, K. An estimate of equatorial upwelling in the Pacific. *J. Phys. Oceanogr.* **11,** 1205–1214 (1981).
32. Meinen, C. S., McPhaden, M. J. & Johnson, G. C. Vertical velocities and transports in the equatorial Pacific during 1993–1999. *J. Phys. Oceanogr.* **31,** 3230–3248 (2001).
33. Guilderson, T. P. & Schrag, D. P. Abrupt shift in subsurface temperatures in the tropical Pacific associated with changes in El Niño. *Science* **281,** 240–243 (1998).
34. Chang, P., Giese, B. S., Ji, L., Seidel, H. F. & Wang, F. Decadal change in the south tropical Pacific in a global assimilation analysis. *Geophys. Res. Lett.* **28,** 3461–3464 (2001).
35. Knutsen, T. R. & Manabe, S. Model assessment of decadal variability and trends in the tropical Pacific Ocean. *J. Clim.* **11,** 2273–2296 (1998).
36. Federov, A. V. & Philander, S. G. H. Is El Niño changing? *Science* **288,** 1997–2001 (2000).
37. Urban, F. E., Cole, J. E. & Overpeck, J. T. Influence of mean climate change on climate variability from a 155-year tropical Pacific coral record. *Nature* **407,** 898–993 (2000).
38. Kirtman, B. P. & Schopf, P. S. Decadal variability in ENSO predictability and prediction. *J. Clim.* **11,** 2843–2822 (1998).
39. Meehl, G. A. & Washington, W. M. El Niño-like climate change in a model with increased CO_2 concentrations. *Nature* **382,** 56–60 (1995).
40. Feely, R. A., Wanninkhof, R., Takahashi, T. & Tans, P. Influence of El Niño on the equatorial Pacific contribution to atmospheric CO_2 accumulation. *Nature* **398,** 597–601 (1999).
41. Feely, R. A. *et al.* Seasonal and interannual variability of CO_2 in the equatorial Pacific. *Deep-Sea Res.* (in the press).
42. Conkright, M. E. *et al. World Ocean Database 1998 Version 2.0* (National Oceanographic Data Center Internal Report 14, National Oceanic and Atmospheric Administration, Silver Spring, Maryland, 1999).
43. da Silva, A. M., Young, C. C. & Levitus, S. *Atlas of Surface Marine Data* Vol. 1, Algorithms and Procedures (NOAA Atlas NESDIS 6, US Dept. of Commerce, Washington DC, 1994).
44. Goldenberg, S. B. & O'Brien, J. J. Time and space variability of tropical Pacific wind stress. *Mon. Weath. Rev.* **109,** 1190–1207 (1981).
45. Kalnay, E. *et al.* The NCEP/NCAR 40-year reanalysis project. *Bull. Am. Meteorol. Soc.* **77,** 437–471 (1996).
46. European Centre for Medium-Range Weather Forecasts – ECMWF Data Archive (http://www.ecmwf.int/services/data/archive/) (February 2001).
47. Hackert, E. C., Busalacchi, A. J. & Murtugudde, R. A. A wind comparison study using an ocean general circulation model for the 1997–98 El Niño. *J. Geophys. Res.* **106,** 2345–2362 (2001).
48. Godfrey, J. S. A Sverdrup model of the depth-integrated flow for the World Ocean allowing for island circulations. *Geophys. Astrophys. Fluid Dyn.* **45,** 89–112 (1989).
49. Schneider, N. The Indonesian throughflow and the global climate system. *J. Clim.* **11,** 676–689 (1998).
50. Smith, T. M., Reynolds, R. W. & Ropelewski, C. F. Optimal averaging of seasonal sea surface temperatures and associated confidence intervals. *J. Clim.* **7,** 949–964 (1994).

Acknowledgements

We thank J. Potemra for advice on Indonesian throughflow calculations. We also thank W. Kessler, G. Johnson and R. Kleeman for comments on an earlier version of this manuscript. This work was supported by the NOAA Office of Oceanic and Atmospheric Research and by the Joint Study for the Atmosphere and Ocean (JISAO) at the University of Washington.

Correspondence and requests for materials should be addressed to M.J.M. (e-mail: mcphaden@pmel.noaa.gov).

© 2002 Macmillan Magazines Ltd